Correlations between the Surface Structure of Platinum Single Crystals and Hydrocarbon Skeletal Rearrangement Mechanisms: Approach to the Nature of the Active Sites

A. DAUSCHER, F. GARIN, AND G. MAIRE

*Laboratoire de Catalyse et Chimie des Surfaces, U.A. 423 du CNRS, Université Louis Pasteur,
4 rue Blaise Pascal, 67070 Strasbourg, France*

The isomerization and hydrocracking reactions of 2-methylpentane and *n*-hexane and the hydrogenolysis of methylcyclopentane were investigated on a clean Pt (311) single crystal at 350°C under atmospheric pressure in an isolation cell housed within an ultrahigh vacuum chamber. The surface composition was monitored before and after the catalytic reactions by Auger electron spectroscopy. The results were compared with those obtained in the same experimental conditions on Pt (111), Pt (557), and Pt (119) surfaces, a polycrystalline foil, and two Pt/Al₂O₃ catalysts of both low and high dispersion. Experiments with labeled hexanes were also undertaken to determine the nature of the mechanisms involved in the isomerization reactions. The catalytic results show that each crystallographic face has its own peculiarities especially for (i) catalytic activity, (ii) selectivity as regards isomers produced, and (iii) selectivity as regards mechanisms. Conversely, the distribution of cracked products presents no significant structure sensitivity on "massive" metal surfaces although the highly dispersed alumina-supported platinum catalysts behave differently. Results with ^{13}C-labeled hydrocarbons suggest that the atoms in the so-called B_5 site configuration are responsible for the bond-shift plus cracking reactions and that the atoms located at the corners and edges are involved in the cyclic mechanism. © 1987 Academic Press, Inc.

INTRODUCTION

Skeletal rearrangement reactions of hexanes have been widely investigated over many types of platinum catalysts. The mechanisms involved in these reactions, i.e., the cyclic (*1*) and bond-shift mechanisms (*2*), are now well characterized using ^{13}C-labeled hydrocarbons (*3*). However, it has not yet been possible to define surely and to characterize the real nature of the active sites associated with each reaction pathway. The use of well-defined surfaces of platinum, for instance, single crystals, of both low and high index, can be helpful in determining the nature of the active sites and also in obtaining more detailed information about the structure sensitivities of alkane skeletal rearrangement reactions. Extensive work on supported platinum catalysts and platinum single-crystal faces has

shown that hydrogenolysis of methylcyclopentane and isomerization of hexanes are very sensitive to surface structure and to metal particle size (*4, 5*). Somorjai and co-workers studied the skeletal rearrangement reactions of isobutane (*6*), *n*-hexane (*7*), and *n*-heptane (*8*). In the *n*-hexane study, only the aromatization reaction displayed structure sensitivity compared with isomerization, C₅-dehydrocyclization, and hydrocracking reactions. Nevertheless, the peculiar catalytic properties of highly dispersed supported platinum catalysts have never been simulated by platinum single-crystal surfaces (4). On the (557) and (119) stepped surfaces the skeletal rearrangement mechanisms of hexanes have been interpreted by different species adsorbed on the edges and near-edge rows of atoms and by taking into account (i) the surface crystallography, the surface diffusion, and the electronic prop-

erties of the platinum atoms, and (ii) the electronic structures of the hydrocarbons (9–12).

Moreover, vicinal faces with (111) or (100) orientations are reconstructed in the presence of hydrogen or traces of oxygen, sulfur, and carbon (13–16). The vicinal faces with (111) terraces undergo surface reconstruction, perhaps induced by a very small amount of sulfur in hydrogen and hydrocarbon mixtures and this enhances the bond-shift mechanism. In the case of the (557) reconstructed surface, the active centers could be attributed to the formation of a new kind of ledge corresponding to a Pt(311) orientation and containing both hydrogen and platinum atoms. Therefore the study of a Pt(311) single-crystal surface was investigated. Moreover, Somorjai (17) showed that this (311) crystallographic orientation is stable under ultrahigh vacuum (UHV) at high temperatures and in the presence of various gases (O_2, CO, etc.). Finally, the (311) orientation is associated with the B_5 sites suggested as being possible active catalytic centers in the incomplete cubooctahedron model proposed by van Hardeveld and van Montfoort (18, 19).

EXPERIMENTAL

Materials

The unlabeled hydrocarbons used were Fluka puriss grade. A purity test of each batch of hydrocarbon was undertaken to avoid any influence of impurity on the product distribution after catalytic reaction. Thus methylcyclopentane which contains 0.07% n-hexane as impurity was purified by gas–liquid chromatography before each experiment. The major impurity of n-hexane is 3-methylpentane (0.14%), but it was considered unreactive on the basis of the amount of 3-methylpentane present after catalytic reaction. The 2- and 3-methylpentanes showed no perceptible impurity by gas–liquid (F.I.D) chromatography and were used as such.

The ^{13}C-labeled hydrocarbons used,

namely 2-[2-^{13}C]methylpentane, 2-[4-^{13}C]methylpentane, and 3-[3-^{13}C]methylpentane, were prepared by synthetic methods already described (20).

Apparatus and Procedure

The experiments on platinum single-crystal and polycrystalline surfaces were performed in a Varian LEED chamber with four-grid optics. A retarding field analyzer (RFA) was used to monitor the surface composition before and after the catalytic reaction. An isolation cell housed within the main UHV chamber allowed catalytic reactions up to atmospheric pressure to be conducted while the rest of the chamber remained under ultrahigh vacuum.

The crystal samples were mounted on tantalum rods and were heated by direct Joule effect. In each run, 5 Torr of hydrocarbon was introduced with 755 Torr of pure hydrogen (Air Liquide, 99.99%). After 1 h of contact time at a controlled temperature (350 ± 5°C), the reaction products were hydrogenated on Adams platinum and then trapped in liquid nitrogen. A fraction of the gas phase was directly analyzed by gas chromatography and a part of the reaction mixture was used for mass spectroscopic location of the ^{13}C in each molecule. More details are given in Ref. (4). The Pt(311) single crystal was cleaned as described elsewhere (15, 21) until Auger electron spectroscopy (AES) revealed a minimum of impurities (C, S, Ca, Si, O). The crystal was cut by spark erosion after orientation with Laue back reflection techniques ($\Delta\theta$ = ±15 min) from the same single-crystal rod (MRC, 99.999%) as the other platinum single-crystal surfaces ((111), (557), (119)).

Two Pt/Al$_2$O$_3$ catalysts were prepared by impregnating chloroplatinic acid onto an inert Woelm alumina, leading to a 0.2 wt% platinum catalyst and a dispersion given by a H/Pt ratio of 1, or onto a Matheson–Coleman alumina leading to a 5 wt% platinum catalyst with a dispersion of 0.2.

The experiments on supported catalysts

were performed in a differential reactor at atmospheric hydrogen pressure. The experimental procedure for the catalytic experiments has already been described (20, 22).

RESULTS

Isomerization and Hydrocracking of 2-Methylpentane (2MP)

The catalytic reactions were undertaken on four platinum single-crystal surfaces, a platinum polycrystalline foil, and two supported platinum catalysts with different metal loadings at 350°C under 760 mm Hg. The overall conversion (% α_T), given for a 1-cm^2 area of platinum, the percentage of selectivity (% S), defined as the percentage (in moles) of C_6 isomers in the reaction products, and several ratios of reaction products are given in Table 1. The peak to peak height ratios $c = h(C)$ 269 eV/h(Pt)233 eV and $e = h(O)$ 510 eV/h(Pt) 167 eV given by AES after catalytic reactions are also noted in Table 1.

No diffusion phenomenon was observed because the overall conversion became greater with increasing reaction time and sample area (23). A small extensive cracking, leading to methane and ethane formation, was obtained and corresponded roughly to 3% of the product distribution. Consecutive reactions can be considered as

negligible as shown by the high isobutane/ n-butane ratios. The values of the n-pentane/isopentane ratios are somewhat lower than 2, the value of a statistical rupture of the C–C bonds, whatever the crystalline face or the supported catalyst.

The platinum polycrystalline foil is four times more reactive than the most reactive platinum single-crystal surface (Pt(557)); Pt(111) is the least reactive. The stepped Pt(557) face possesses also the highest isomerization power (S = 72%), whereas Pt(119) is the most cracking surface (S = 43%). Although the percentage of cracked products is different on each surface, the distributions of cracked products are the same, as shown by the demethylation/deethylation and demethylation/internal-rupture ratios. The supported platinum catalyst of low dispersion behaves like the crystalline surfaces while the one of high dispersion has a completely different behavior.

The 3-methylpentane/n-hexane ratio varies between 1.1 for the Pt(111) surface and 2.1 for the stepped Pt(557) surface. It never reaches the very low value obtained on the highly dispersed catalyst. The formation of benzene is predominant on the Pt(311) surface followed by the Pt(119) surface. The other platinum single or polycrystalline surfaces as well as the supported catalysts do

TABLE 1

Isomerization and Hydrocracking of 2-Methylpentane at 350°C under a Total Pressure of 760 Torr[a]

Catalyst	% α_T	% S_i	nP/iP	iB/nB	$\frac{C_1 + C_5}{C_2 + C_4}$	$\frac{C_1 + C_5}{2C_3}$	3MP/nHx	$\frac{Bz + cHx}{MCP}$	$\frac{MCP + Bz + cHx}{3MP + nHx}$	AES ratios[b] c	e
5% Pt/Al$_2$O$_3$	2.8	94.2	1.8	5.0	0.9	1.0	1.9	0	1.0	—	—
0.2% Pt/Al$_2$O$_3$	3.4	92.7	1.9	10.0	2.0	2.7	0.4	0.01	0.9	—	—
Pt(557)	0.9	72.3	2.0	13.3	0.7	1.0	2.1	0	1.5	0.95	0.10
Pt(111)	0.2	53.5	1.7	2.6	—	—	1.6	0.03	4.9	1.20	0.20
Pt(119)	0.5	43.4	1.7	5.6	0.5	0.6	1.1	0.17	3.2	1.22	0.20
Pt(311)	0.6	59.3	1.7	3.6	0.4	0.5	1.4	0.33	2.5	1.50	0.24
Pt polycryst.	3.2	69.9	1.5	5.0	0.5	0.6	1.4	0	1.6	2.30	0.20

[a] nP/iP = n-pentane/isopentane; iB/nB = isobutane/n-butane; 3MP/nHx = 3-methylpentane/n-hexane; Bz + cHx/MCP = benzene + cyclohexane/methylcyclopentane.
[b] Auger electron spectroscopy results. $c = h(C)$269 eV/h(Pt) 233 eV; $e = h(O)$ 510 eV/h(Pt) 167 eV after catalytic reaction. Before any catalytic reaction, $c = e = 0$.

not lead to a significant formation of benzene. The cyclic-isomers/acyclic-isomers ratio is the highest for the flat (111) surface where the overall conversion is the lowest. The Pt(311) surface has its own catalytic behavior (activity, selectivity, product distribution).

Isomerization and Hydrocracking of n-Hexane

In Table 2 are reported the results obtained for the Pt(311) single-crystal surface and the platinum polycrystalline foil. Experiments 1 and 2 give the reaction product distribution after 1 and 2 h of reaction time, respectively. Experiment 3 relates to 1 h of reaction time but was undertaken in another UHV apparatus. Experiments 1 and 3 (1 h of contact time) show the reproducibility of the results. The distributions are compared with those obtained by Somorjai and co-workers (7) on a Pt(100) single crystal at 350°C and under a total pressure of 620 Torr.

The overall conversion is the same after 1 or 2 h of reaction time on the platinum foil if the latter is referenced to 1 h. On the other hand, the 2-methylpentane/3-methylpentane ratios, the percentage of isomerization selectivity, and the demethylation reactions decrease after longer reaction time. The distribution in the cyclic isomers does not vary.

After 1 h of reaction time, the platinum (311) single crystal is four times less reactive than the platinum foil while the selectivity is roughly the same. The Pt(311) surface presents a low contribution in demethylation reactions. The 1–6 ring closure and more generally the ring closures 1–6 and 1–5 are much more important on the Pt(311) single crystal than on the platinum polycrystalline foil when compared with acyclic isomerization. The Pt(100) single-crystal surface shows a higher selectivity to isomers and a less important 1–6 ring closure reaction than the other surfaces. This face differs essentially by its very low 2MP/3MP ratio.

Hydrogenolysis of Methylcyclopentane

The results obtained at 350°C under atmospheric hydrogen pressure are reported in Table 3. Some extensive cracking reactions were observed on single crystals, especially on the Pt(111) and Pt(311) faces. The 2-methylpentane/3-methylpentane ratios (2.3 ± 0.3) can be roughly considered constant whatever the plane is used. They are somewhat higher on supported catalysts. A value of 0.5 for the 3-methylpentane/n-hexane (nHx) ratio is characteristic of a highly dispersed supported platinum catalyst. This value is observed on Pt(311) and has never been obtained before on platinum single-crystal surfaces.

TABLE 2

Isomerization and Hydrocracking of n-Hexane at 350°C under a Total Pressure of 760 Torr after 1 h Reaction Time

Catalyst	Expt. No.	% α_T	% S	$\dfrac{C_1 + C_5}{C_2 + C_4}$	$\dfrac{C_1 + C_5}{2C_3}$	$\dfrac{2MP}{3MP}$	$\dfrac{Bz + cHx}{MCP}$	$\dfrac{MCP + Bz + cHx}{3MP + 2MP}$	AES ratios	
									c	e
Pt(311)		0.5	61.3	0.5	0.3	1.5	0.4	2.8	1.8	0
Pt polycryst.	1	2.3	65.2	1.1	0.8	1.7	0.2	2.9	—	—
Pt polycryst.[a]	2	4.1	53.5	0.8	0.7	1.2	0.3	1.7	1.5	0.13
Pt polycryst.[b]	3	1.9	65.8	0.6	0.6	1.8	0.25	1.8	3.3	0.22
Pt(100)[c]		—	76.9	0.4	0.4	0.7	0.10	2.6	—	—

[a] After 2 h of reaction time, unpublished results Zielinsky et al. (23).
[b] Experiment in another UHV apparatus.
[c] Ref. (7), total pressure = 620 Torr.

TABLE 3

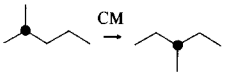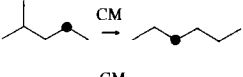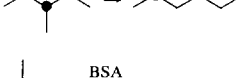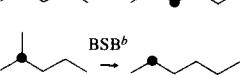Hydrogenolysis of Methylcyclopentane at 350°C and 760 mm Hg
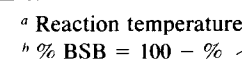
Catalyst	% α_T	% Cracking	$\dfrac{2MP}{3MP}$	$\dfrac{3MP}{nHx}$	$\dfrac{nHx}{Bz + cHx}$	AES ratio	
						c	e
5% Pt/Al$_2$O$_3$	10.0	0	3.2	1.8	10.4	—	—
0.2% Pt/Al$_2$O$_3$	5.8	6	2.9	0.5	6.4	—	—
Pt(557)	2.8	3	2.7	1.5	6.3	—	—
Pt(111)	0.3	40.5	2.0	3.0	3.7	1.3	0.2
Pt(311)	1.0	46	2.3	0.5	3.3	1.9	0.7
Pt polycryst.	5.0	7	2.2	1.3	46	2.6	0.1

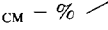## Isomerization of Labeled C$_6$ Hydrocarbons

The isomerization reactions of 2-[2-^{13}C],2-[4-^{13}C]-, and 3-[3-^{13}C]methylpentanes have been studied at 350°C under a total pressure of 760 Torr on supported catalysts, single crystals, and a polycrystalline foil. In Table 4 are reported the distributions of the observed isotopic varieties and the relative percentages of cyclic and bond-shift mechanisms. The detailed method of determining the different contributions are explained in Ref. (20). Pt(311) gave a cyclic mechanism contribution of 42% in the 2MP → 3MP reaction. This value is near those found for the Pt(119) and polycrystalline surfaces but is clearly higher than for a Pt(557) face. It is also between the contributions observed for a well-dispersed supported catalyst (76%) and a poorly dispersed one (34%). The cyclic mechanism

TABLE 4

Isomerization of 2-[2-^{13}C], 2-[4-^{13}C], and 3-[3-^{13}C]Methylpentanes at 350°C at Atmospheric Hydrogen Pressure

Catalyst	5% Pt/Al$_2$O$_3$	0.2% Pt/Al$_2$O$_3$[a]	Pt(311)	Pt(557)	Pt(119)	Pt polycryst
Dispersion = H/Pt	0.2	1				
CM (1)	34	76	42	14	39	49
CM (2)	72	86	68	70	—	65
CM (3)	61	90	71	51	—	64
BSA	10	5	14	21	30	13
BSB[b]	18	9	18	9	—	22

[a] Reaction temperature = 390°C (Ref. (24)).

[b] % BSB = 100 − % CM − % BSA.

contribution in chain lengthening is similar on all crystalline faces and on the poorly dispersed supported catalyst either in the 2MP → nHx reaction or in the 3MP → nHx reaction. The A and B bond-shift contributions on Pt(311) are similar to those obtained on a platinum polycrystalline foil and a supported catalyst of low dispersion. The methyl migration (BS A) is lower on Pt(311) compared to that on the stepped Pt(557) or Pt(119) surface, while the propyl migration (BS B) is more important.

The quantity of 3-methylpentane obtained by a cyclic mechanism (CM) or a bond-shift (BS) mechanism can be calculated by knowing the relative contributions of cyclic and bond-shift mechanisms, respectively. The same can be calculated for n-hexane. Thus the sum of cyclic mechanism products represents the 3MP and nHx obtained by the cyclic mechanism as well as the methylcyclopentane (MCP), the benzene, and the cyclohexane. The sum of bond-shift products represents the 3MP and nHx obtained only by a bond-shift mechanism. These calculations are reported in Table 5.

The ΣCM/ΣBS ratios vary between 2.6 for the Pt(557) surface and 9.0 for the Pt(111) surface, and reaches a value of 45 for the highly dispersed supported platinum catalyst, though the value of MCP/(3MP + nHx)$_{CM}$ is very low. This clearly shows that

the presence of methylcyclopentane in the product distribution is not only an indication of the cyclic mechanism. The rates to hydrogenolyze the methylcyclopentane intermediate are sometimes higher than the desorption rates, leading to higher contributions of 3-methylpentane and n-hexane obtained via a cyclic mechanism and to a lower contribution of methylcyclopentane.

As the same intermediate of reaction is involved in both cracking and bond-shift reactions (3) the former can be considered as parallel reactions to bond shift. If we sum the contributions of the bond-shift and cracking reactions, the ΣCM/Σ(crack. + BS) ratios (Table 5) are constant whatever the crystal surface used and equal to 1.1 ± 0.1, except for the (119) face where this ratio is equal to 0.6. On supported catalysts, values of 2.4 and 10.3 are found for the 5% Pt/Al$_2$O$_3$ and 0.2% Pt/Al$_2$O$_3$ catalysts, respectively. On the other hand the Σcrack./ΣBS ratio increases from 1.5 on the (557) face to 12.5 on the (119) face, these two surfaces having terraces of (111) and (100) orientations, respectively.

DISCUSSION

The study of the different platinum surfaces clearly shows an important structural effect. In fact, the catalytic behavior of each face has its own character, the reproducibility being verified on two different

TABLE 5

Product Distribution from 2-Methylpentane as Determined by ^{13}C Measurements

| Catalyst	% α_T (moles)	% Cracking	$\dfrac{MCP}{(3MP + nHx)_{CM}}$	$\dfrac{\Sigma CM}{\Sigma BS}$	$\dfrac{\Sigma CM}{\Sigma BS + \Sigma CM}$	$\dfrac{\Sigma crac.}{\Sigma BS}$ (ratio B)	$\dfrac{\Sigma CM}{\Sigma BS + \Sigma crac.}$ (ratio A)
5% Pt/Al$_2$O$_3$[a]	2.8	6	2.4	2.9	75	0.2	2.4
0.2% Pt/Al$_2$O$_3$[a]	3.4	7	0.9	45.5	98	3.4	10.3
Pt(557)	0.9	27.5	4.5	2.6	72.5	1.5	1.1
Pt(119)	0.5	57	6	8.3	89.5	12.5	0.6
Pt(111)[b]	0.2	45	11	9.0	90	8.0	1.0
Pt(311)	1.1	43	2	6.0	86	5.0	1.0
Pt polycryst.	1.7	35.5	3.5	5.7	85	3.5	1.2

[a] For the physical characterizations of these catalysts, see Ref. (5).
[b] on Pt(111), α_T being very low, ΣCM/ΣBS ~[MCP]/ΣBS.

sets of experimental apparatus. Moreover, the behavior of a highly dispersed catalyst is different from one with a pure metallic character.

Catalytic Activities

The total activity for both reactions of hydrogenolysis of methylcyclopentane and isomerization of 2-methylpentane decreases in the following order:

Pt polycrystalline > Pt(557) > Pt(311)

> Pt(119) > Pt(111)
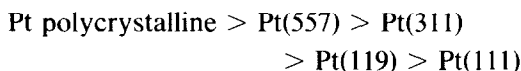
Considering the activities on the reconstructed (557) and on the (311) faces, the latter does not show a higher reactivity. This can be due to the fact that the rows of atoms on the topmost layer are too close one to another and provide steric hindrance to hydrocarbon adsorption. From these catalytic activities we can assume that the combination of atoms on (111) terraces, which can be considered as hydrogenation–dehydrogenation sites or adsorption sites, and atoms on the ledges, which are the reactive ones, is necessary to obtain highly reactive surfaces.

Catalytic Selectivities

Under constant reaction conditions, the catalytic selectivities change significantly as a function of the structure of the well-characterized Pt surfaces. The percentage of cracked products for the 2-methylpentane reactions (Table 5) is higher on the Pt(119) surface and lower for Pt(557), which is in good agreement with the results of Davis et al. (7) for the hydrocracking reactions of n-hexane. The Pt (13, 1, 1) surface with (100) terraces displayed a greater cracking power. On the other hand, the (10, 8, 7) surface with (111) terraces and kinked steps leads to fewer carbon–carbon ruptures. Gillespie et al. (8) also found that the Pt(557) face was the surface less susceptible to cracking for the n-heptane reactions. Nevertheless, the flat Pt(100) surface does not present this cracking character. It arises from these results that the most hy-

drocracking sites are an association of a (100) crystallographic arrangement with a (111) one for a hydrocarbon previously dehydrogenated on (100) terraces. In our case, the high percentage found on the Pt(311) surface for the methylcyclopentane reaction could be due to the important amount of oxygen often detected, with silicon diffusing from the bulk during the catalytic reaction. It is well known that in the presence of oxygen, the percentage of cracked molecules is enhanced (8, 25, 26).

In Fig. 1 are shown the modes of cracking of 2-methylpentane on several crystal faces and Pt/Al$_2$O$_3$ catalysts. It appears that the 2-methylpentane hydrocracking exhibits no significant structure sensitivity. The deethylation reactions are always the most important whatever the face, these reactions being thermodynamically favored at 350°C. Conversely, Davis et al. (7) found some differences in the cracking modes for n-alkanes among the several faces studied. Nevertheless, our results for n-hexane on Pt(311) and polycrystalline Pt (Table 2) are quite similar to those obtained on Pt(100) by Davis et al. (7). Although the platinum polycrystalline foil possesses single-crystal grains of (111) orientation as detected by LEED (4), it behaves like the (100) face.

The demethylation/deethylation ratios for the 2-methylpentane reactions are ap-
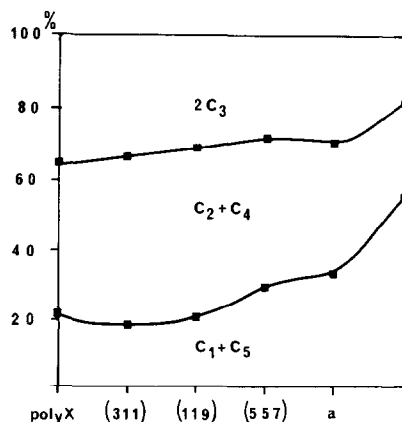

FIG. 1. Distribution of cracked products from 2-methylpentane at 350°C and 760 Torr (a = 5% Pt/Al$_2$O$_3$, b = 0.2% Pt/Al$_2$O$_3$).

proximately equal to 0.5 ± 0.1 on the single crystals, 0.7 ± 0.1 on the Pt/Al₂O₃ catalyst of low dispersion, and 0.6 ± 0.1 on Pt black catalysts (25). This is typical of a metallic character. The value of 2.0 ± 0.2 found for the highly dispersed Pt/Al₂O₃ catalyst shows that small particles apparently do not keep a really metallic character and emphasizes the importance of metal–support interactions. The supports may influence essentially the electronic properties of the finely divided metal and through them the catalytic properties. It has been proposed that small particles supported on alumina or on zeolites present an electron-deficient character (27, 28) while when supported on titanum dioxide they present an excess electron character (29, 30). Another possible explanation could be the adlineation model proposed by Glassl et al. (31). These results are in perfect accordance with the kinetic data obtained for pentanes on poorly and highly dispersed platinum catalysts. The activation energy for the deethylation reactions is higher than that for the demethylation ones on large metallic particles but is similar to that on small crystallites (32, 33). The results obtained with 3-methylpentane corroborate the ones obtained with 2-methylpentane (34).

The isomer product distribution is shown in Fig. 2 for the different faces and sup-
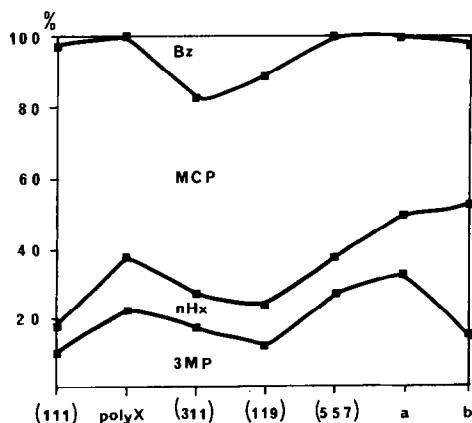

FIG. 2. Isomer product distribution from 2-methylpentane at 350°C and 760 Torr (a = 5% Pt/Al₂O₃, b = 0.2% Pt/Al₂O₃).

ported catalysts studied for the 2-methylpentane reactions at 350°C under atmospheric hydrogen pressure. The relative contribution of n-hexane among the isomer products seems not to be structure dependent except for the 0.2% Pt/Al₂O₃ catalyst which has, again, a peculiar behavior.

The 3-methylpentane, methylcyclopentane, and benzene formations are, conversely to n-hexane formation, dependent on the surface structures of the single crystals. The selectivity in 3MP isomerization is greatest on the Pt(557) surface and on the platinum polycrystalline foil but the reaction occurs essentially either via a bondshift mechanism or via a cyclic mechanism, respectively, as shown in Table 4. The Pt(119) surface shows a lower isomerization power. This is in contradiction to the results obtained with isobutane as reactant hydrocarbon by Davis et al. (6) who claimed that the (100) stepped surfaces are better isomerization catalysts. In fact, these results were not reproducible with n-hexane (7). It is worthwhile to notice that for small molecules no cyclic mechanism can occur. The percentage of methylcyclopentane in the reaction products changes erratically. This can be explained by its close dependence upon overall conversion (1).

Benzene formation is favored on Pt(311) and Pt(119) single-crystal surfaces. The Pt(557) and Pt(111) surfaces do not lead to any formation of benzene even at 350°C. Conversely, Davis et al. (7) found that the aromatization reaction, when starting with n-hexane, was favored on Pt crystals with (111) orientations and was comparatively lowered on (100) terraces. Nevertheless, the benzene formation cannot occur by a direct mechanism when starting with 2-methylpentane. On Pt(311), the benzene + cyclohexane contributions obtained during the hydrogenolysis of methylcyclopentane are lower (~5% of the total products) than those obtained by aromatization of 2-methylpentane and n-hexane (~10%). Opposite results are obtained on the other

platinum faces and on supported catalysts. The 1–5 into 1–6 ring enlargement seems to be disfavored on the Pt(311) surface compared to direct 1–6 ring closure. Nevertheless, benzene formation is no greater for *n*-hexane, where this cyclization is direct, than for 2MP where the cyclization can only occur after a skeletal rearrangement. The 1–6 ring closure would therefore be a slow pathway while the 2MP → nHx rearrangement would be fast.

The high contribution of benzene in the product distribution on the Pt(311) single crystal could be explained by supposing that (i) the adsorbed benzene molecule is not parallel to the surface and (ii) the adsorption strengths are weaker. Moreover, the formation of olefins is favored on the Pt(311) surface compared with the other single crystals, this crystallographic orientation having therefore poorly rehydrogenating sites.

During the hydrogenolysis of methylcyclopentane (Table 3), important hydrocracking reactions occurred on the Pt(111) and Pt(311) surfaces. As the alkane activities are the same, the cracking rates of 2-methylpentane, 3-methylpentane, and *n*-hexane can be supposed similar. Consequently the values obtained for the different ratios (2MP/3MP and 3MP/nHx) in the methylcyclopentane hydrogenolysis reflect initial distributions. High values (1.3 to 3.0) of the 3MP/nHx ratios are obtained on Pt(111) and Pt(557) faces, Pt polycrystalline foil, and poorly dispersed supported catalysts while low values, equal to 0.5, are obtained on the Pt(311) face and also on highly dispersed catalysts. Again, in the labeled experiments, a value of 0.8 was obtained for the 3MP/nHx ratio on the (311) surface, these two hydrocarbons being derived from the hydrogenolysis of the methylcyclopentane reaction intermediate. After both reactions of hydrogenolysis of methylcyclopentane and isomerization of 2-[2-^{13}C]methylpentane, oxygen was detected by AES, the ratio *e* being 0.7 and 0.2, respectively. The presence of small amounts

of oxygen could be responsible for the observed distributions.

Approach to the Nature of the Active Sites

As the specific rates of isomerization seem to be structure insensitive (*35*) while the selectivity in mechanisms is structure sensitive on platinum catalysts, it is necessary to consider that weakly adsorbed species are precursors of strongly adsorbed ones and the following sequence of elementary reactions arises (Fig. 3):

(1) indiscriminate adsorption of a gaseous molecule on a face atom of the metal crystallite to form a weakly adsorbed molecule: all the surface atoms can be considered as potential adsorption sites (S_A);

(2) surface migration from the adsorption site S_A to a reactive site S_R located on some specific region of the metal particle (ledges, edges, defects, corners);

(3) formation on the reactive site of a highly dehydrogenated species whose migration capacity is very low;

(4) skeletal rearrangement of this strongly adsorbed species; and

(5) rehydrogenation of the strongly adsorbed entity, surface migration, and desorption of the weakly adsorbed isomerized molecule (reverse of steps 3, 2, and 1), to yield the reaction product.

In Table 6 are summarized the various structural and mechanistic observations made on the different catalysts.

For small metal crystallites, the surface atoms have a low average coordination number and the adsorption sites S_A are the same as the reactive sites S_R. Consequently, competition between carbon–carbon bond recombination and desorption of the reaction intermediates will occur (*3*). The cracked products are favored, the ratio $B = \Sigma crack./\Sigma BS$ being equal to 3.4 (Table 5). The ratio $A = \Sigma CM/\Sigma crack. + \Sigma BS$ is high ($A = 10$), indicating a large predominance of cyclic mechanism. However, on these crystallites whose metal particles size

TABLE 6

Relationship between the Mechanisms and the Nature of the Active Sites

Catalyst	Existence of B_5 sites (18)	Mechanisms (see Table 5)		Sites[a]
0.2% Pt/Al$_2$O$_3$	No	crack. $\gg$ BS	CM $\gg$ BS + crack.	$S_A = S_R$
5% Pt/Al$_2$O$_3$	Yes	crack. $\ll$ BS	CM $>$ BS + crack.	$S_R > S_A$
Pt(311)	Yes	crack. $>$ BS	CM $=$ BS + crack.	$S_A = S_R$
Pt(557)	Yes	crack. $\sim$ BS	CM $=$ BS + crack.	$S_A > S_R$
Pt(111)	Yes (defects)	crack. $>$ BS	CM $=$ BS + crack.	S_A "work" $> S_R$
Pt(119)	Yes	crack. $\geqslant$ BS	CM $<$ BS + crack.	
Pt polycryst	Yes (defects)	crack. $>$ BS	CM $=$ BS + crack.	S_A "work" $> S_R$

[a] Availability of the adsorption and reactive sites S_A and S_R.

is smaller than 1.0 nm (5), no B_5 sites as defined by van Hardeveld and van Montfoort (18) are present. The presence of B_5 sites on the surface can therefore be considered as responsible for the bond-shift and/or cracking reactions.

On the Pt(311) surface, the amount of S_A sites is similar to the amount of S_R sites. Hence, the cracked products are favored compared to the bond-shift isomerized product (ratio $B = 5$). B_5 sites are present and the ratio A is lower ($A = 1$) than on small particles. This clearly shows that the cracking and bond-shift reactions are initiated on the B_5 sites. The presence of olefins on this face can be easily understood by the fact that $S_A \sim S_R$; the surface migration (reaction (5)) is not complete and the products are readily released in the gas phase after the reactive reaction (reaction (4)).

On the Pt(557) face the adsorption sites S_A are in excess compared to the reaction sites S_R. Isomerization reactions are therefore favored compared to cracking ones ($B = 1.5$). Moreover, the (557) surface is reconstructed under hydrogen and leads to reactive steps with (311) orientations which imply the presence of more accessible B_5 sites and the A ratio is equal to 1.

The Pt(111) surface leads to a high B ratio ($B = 8$). We suppose that the adsorption sites which are really working (assigned as step 3 in Fig. 3) are few compared to the overall surface because the catalytic activ-

ity is very low. S_A (working) $\sim S_R$ and the cracking reactions are increased because the recombination is disfavored. On the other hand, the ensembles $S_A + S_R$ involved in the catalytic reaction may have B_5 site orientations which could explain the value of 1 observed for the A ratio.

The Pt(119) face presents a different behavior. The cracking reactions are very important compared to the bond-shift reactions ($B = 12$) and the amount of bond shift + cracking is more important than the cyclic mechanism ($A = 0.6$). At first sight, these results are difficult to explain, the (119) face presenting also B_5 sites along the steps. We believe there is a difference due to (i) the nature of the crystallographic orientations (the (119) surface is a stepped (100) face), (ii) the availability of hydrogen along the different ledges when comparing the reconstructed (557) and the (119) faces, and (iii) the nature of the active sites which are composed of different platinum and hydrogen atoms (36). Consequently, the reactive and adsorption sites must be topographically similar for the (119) face.

The polycrystalline foil behaves like the (311) and (557) faces, but due to the great number of possible orientations and defects it is not possible to establish a direct correlation with S_A and S_R.

Finally, under our experimental conditions, it seems that the amount of cyclic mechanism is very often equal to the contri-
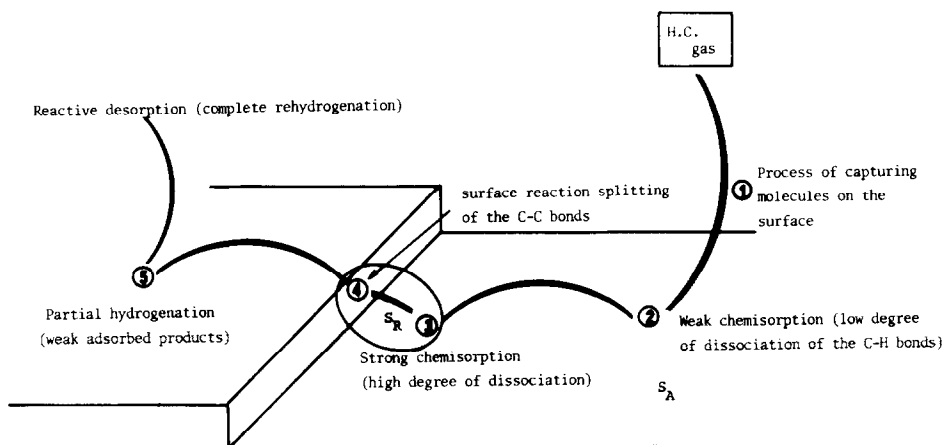
FIG. 3. Elementary reactions occurring in skeletal rearrangements of hydrocarbons on platinum catalysts.

bution of bond shift plus cracking. Taking into account the fcc cubooctahedron model with the incomplete shell, suggested by van Hardeveld and Hartog (*19*), we observe that the ratios between the atoms involved in the B_5 sites and the atoms on the edges (N_E) and corners (N_C) are equal to 37.8 and 39.7 if the total numbers of atoms N_T are 1529 and 124,784, respectively. The limiting value is 40 for this ratio ($N_{B_5} \times 100/N_E + N_C + N_{B_5}$). Our results would suggest that the atoms in the B_5 sites are responsible for the bond-shift and cracking reactions and that the atoms located at the corners and edges are involved in the cyclic mechanism.

CONCLUSIONS

The studies of skeletal rearrangement reactions on various platinum single-crystal surfaces have shown that each crystallographic orientation has its own catalytic behavior for the isomerization or hydrogenolysis reactions of hexanes. The behavior of a supported platinum Pt/Al_2O_3 of low dispersion can be well simulated by such platinum surfaces.

The hydrocracking reactions of hexanes exhibit no significant structure sensitivities. Nevertheless, the ratio of demethylation to deethylation reactions is equal to 0.6 ± 0.2 which is characteristic for metallic charac-

ter in platinum. On well-dispersed platinum particles, the influence of the support (Al_2O_3) becomes important. Our results clearly show that for hydrocarbon reactions in the presence of hydrogen the more active sites are a combination of atoms on (111) terraces and atoms on ledges, while the conditions for more cracking are an association of atoms of (100) and (111) orientations when the hydrocarbon is previously dehydrogenated on a (100) terrace. The results can be explained by the nature of the adsorption and reactive sites.

Surprisingly, the total amount of cyclic mechanism measured with labeled experiments is equal to the amount of bond-shift mechanism plus cracking reactions in the presence of the so-called B_5 sites. On the other hand, on small particles mostly constituted of edges and corners atoms where the B_5 sites could not exist, the cyclic mechanism is predominant. Thus the cracking and bond-shift reactions occur on atoms in the B_5 configuration and the cyclic mechanism on atoms located on corners and edges.

REFERENCES

1. (a) Barron, Y., Maire, G., Cornet, D., and Gault, F. G., *J. Catal.* **2**, 156 (1963); (b) Barron, Y., Maire, G., Muller, J. M., and Gault, F. G., *J. Catal.* **5**, 428 (1966).
2. Anderson, J. R., and Avery, N. R., *J. Catal.* **2**, 542 (1963); *J. Catal.* **5**, 446 (1966).
3. Gault, F. G., *in* "Advances in Catalysis" (D. D. Eley, H. Pines, and P. B. Weisz, Eds.), Vol. 30, p. 1. Academic Press, New York, 1981.
4. Garin, F., Aeiyach, S., Légaré, P., Maire, G., *J. Catal.* **77**, 323 (1982).
5. Dartigues, J. M., Chambellan, A., Corolleur, S., Gault, F. G., Renouprez, A., Moraweck, B., Bosch-Giral, P., and Dalmai-Imelik, G., *Nouv. J. Chim.* **3**, 591 (1979).
6. Davis, S. M., Zaera, F., and Somorjai, G. A., *J. Amer. Chem. Soc.* **104**, 7453 (1982).
7. Davis, S. M., Zaera, F., and Somorjai, G. A., *J. Catal.* **85**, 206 (1984).
8. Gillespie, W. D., Herz, R. K., Pertersen, E. E., and Somorjai, G. A., *J. Catal.* **70**, 147 (1981).
9. Maire, G., and Garin, F., *in* "Catalysis" (J. R. Anderson and M. Boudart, Eds.), Vol. 6, p. 161. Springer Verlag, Berlin, 1984.
10. Jardin, J. P., Desjonquères, M. C., and Spanjaard, D., *J. Phys. C, Solid State Phys.* **18**, 1767 (1985).
11. (a) Popple, J. A., and Gordon, M., *J. Amer. Chem. Soc.* **89**, 4253 (1967); (b) Hall, L. H., and Kier, L. B., *Tetrahedron* **33**, 1953 (1977).
12. Hoffman, R., *J. Chem. Phys.* **39**, 1399 (1963).
13. Lang, B., Joyner, R. W., and Somorjai, G. A., *Surf. Sci.* **30**, 454 (1972).
14. Lanzillotto, A. M., and Bernasek, S. L., *J. Chem. Phys.* **84**, 3553 (1986).
15. Maire, G., Bernhardt, P., Légaré, P., and Lindauer, G., *in* "Proceedings, VII Int. Vac. Congress and IIIrd Int. Conf. on Solid Surface, Sept. 1977, Vienna," (R. Dobrozensky, F. Rüdenauer, F. P. Viehböck, and A. Breth, Eds.), p. 861, 1977.
16. Lindauer, G., Légaré, P., and Maire, G., *Surf. Sci.* **126**, 301 (1983).
17. Somorjai, G. A., *in* "Advances in Catalysis" (D. D. Eley, H. Pines, and P. B. Weisz, Eds.),

Vol. 26, p. 1. Academic Press, New York, 1977.
18. van Hardeveld, R., and van Montfoort, A., *Surf. Sci.* **4**, 396 (1966).
19. van Hardeveld, R., and Hartog, F., *Surf. Sci.* **15**, 189 (1969).
20. Corolleur, C., Corolleur, S., and Gault, F. G., *J. Catal.* **24**, 385 (1972).
21. (a) Lang, B., Légaré, P., and Maire, G., *Surf. Sci.* **47**, 89 (1975); (b) Carrière, B., Légaré, P., and Maire, G., *J. Chem. Phys.* **71**, 355 (1977).
22. Garin, F., and Gault, F. G., *J. Amer. Chem. Soc.* **97**, 4466 (1975).
23. Zielinsky, P., Garin, F., Zyade, S., Maire, G., and Frennet, A., to appear.
24. Dauscher, A., Luck, F., Garin, F., and Maire, G., Metal-Support and Metal-Additive Effects in Catalysis (B. Imelik *et al.*, Eds.), p. 113. Elsevier, Amsterdam, 1982.
25. Luck, F., Doctorat d'Etat (Ph. D.), Strasbourg (1983).
26. Aeiyach, S., Doctorat d'Etat (Ph. D.), Strasbourg (1982).
27. Gallezot, P., Weber, R., Dalla Betta, R. A., and Boudart, M., *Z. Naturforsch. A* **34**, 40 (1979).
28. Vedrine, J. C., Dufaux, M., Naccache, C., and Imelik, B., *J. Chem. Soc. Faraday Trans. I* **74**, 440 (1978).
29. Fung, S. C., *J. Catal.* **76**, 225 (1982).
30. Tauster, S. J., and Fung, S. C., *J. Amer. Chem. Soc.* **100**, 170 (1978).
31. Glassl, H., Kramer, R., and Hayek, K., *in* "Proceedings, 4th Int. Conf. on Solid Surf. and 3rd Europ. Conf. on Surf. Sciences, Cannes" (D. A. Degras and M. Costa, Eds.), p. 533. Soc. Franc. du Vide, Paris, 1980.
32. Garin, F., Gault, F. G., and Maire, G., *Nouv. J. Chim.* **5**, 553 (1981).
33. Garin, F., Maire, G., and Gault, F. G., *Nouv. J. Chim.* **5**, 563 (1981).
34. Dauscher, A., unpublished results.
35. Chambellan, A., Dartigues, J. M., Corolleur, C., and Gault, F. G., *Nouv. J. Chim.* **1**, 41 (1977).
36. Besocke, K., Krahl-Urban, B., and Wagner, H., *Surf. Sci.* **68**, 39 (1977).